Precursors and Transition to Chaos in a Quantum Well in a Tilted Magnetic Field

G. Müller,* G. S. Boebinger, H. Mathur, L. N. Pfeiffer, and K. W. West
AT&T Bell Laboratories, 600 Mountain Avenue, Murray Hill, New Jersey 07974
(Received 4 August 1994; revised manuscript received 26 May 1995)

The discovery of a distinct transition from integrable to chaotic electron dynamics results from resonant tunneling spectroscopy of a quantum well in a tilted magnetic field. The tunneling spectra show peak doubling regions at small tilt angles, which give way to peak tripling at larger tilt angles. The transition to chaos is mapped systematically (by varying bias voltage, magnetic field, tilt angle, and the width of the quantum well). We find that peak doubling (tripling) results from bifurcation (trifurcation) of the dominant stable periodic orbit. These are precursors of the chaos transition.

PACS numbers: 73.20.Dx, 05.45.+b, 73.40.Gk

Despite great theoretical interest, there are relatively few experimental studies of simple quantum systems whose classical counterparts exhibit chaotic dynamics [1]. The first such experiments probed highly excited Rydberg atoms via optical spectroscopy [2]. More recent experiments probe the influence of chaos on the magnetotransport of various semiconductor microstructures (antidot arrays [3] and stadium shaped cavities [4]). Subsequent experiments by Fromhold *et al.* [5] have introduced a new quantum system for chaology: the wide quantum well in a tilted magnetic field. Using resonant tunneling spectroscopy, they studied chaotic dynamics at a fixed magnetic field of sufficient intensity such that the quantum well was in a completely chaotic regime [5,6]. Shepelyansky and Stone [6] have related this system to several well-studied models exhibiting a transition to chaos and obtained criteria for the onset of chaos with increasing tilted magnetic field.

In this Letter, we report the first observation of a distinct transition from regular to chaotic dynamics in a quantum well. By systematically varying the three *in situ* experimental parameters of bias voltage, magnetic field, and tilt angle, we map the parabolic magnetic field dependence of the transition. Poincaré section calculations identify the precursors of the chaos transition as the bifurcation and trifurcation of stable periodic orbits. Data from four samples of different well widths establish the classical scaling of these phenomena. We conclude that quantum wells provide a particularly clear manifestation of the transition from order to chaos, which results from the breakup of stable orbits.

A high-mobility quantum well can be an excellent quantum mechanical realization of a simple classical model which exhibits a transition to chaos. This model consists of a charged particle bouncing specularly off two parallel hard walls, while moving under the influence of constant electric and magnetic fields. Molecular beam epitaxial growth of quantum wells yields atomically precise hard wall confinement. This is in contrast to the semiconductor microstructures whose geometry is determined by lithographically defined gates. Integrability in any system can be unintentionally destroyed by irregularities in the confining potential. The quantum well is integrable when the magnetic field is perpendicular to the confining walls. Three tunable experimental parameters drive the system towards chaos: For example, at a nonzero tilt angle, the system becomes increasingly chaotic with increasing magnetic field. Our sample is a high-mobility GaAs quantum well confined between two layers of AlAs. The "hard walls" are provided by the large conduction band discontinuity between the two materials. Figure 1 depicts the conduction band edge profile for our double barrier tunneling samples under a positive bias voltage U. The bias creates a degenerate two-dimensional electron gas (2DEG) emitter adjacent to the first AlAs barrier with only one confinement subband occupied. This acts as a source of nearly monoenergetic electrons which tunnel into the quantum well. In this experiment, we study quantum wells of thickness $d = 400$, 600, 850, and 1200 Å. Unwanted accumulation of charge in the quantum well is avoided by making the second AlAs barrier substantially thinner than the first (37 compared to 57 Å). Also, the quan-

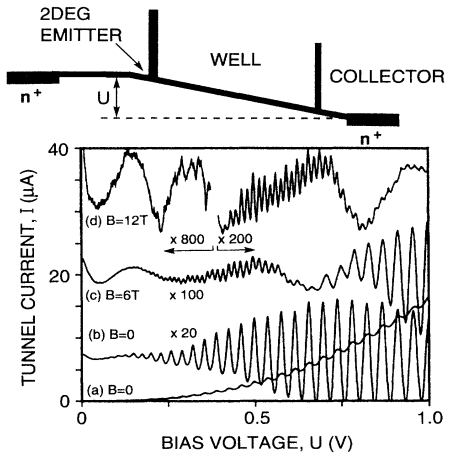

FIG. 1. Schematic conduction band profile of the resonant tunneling sample under bias voltage U. Below are representative current-voltage traces of the 1200 Å sample taken at tilt angle $\theta = 27°$ for $T = 1.5$ K and total magnetic field $B = 0$, 6, and 12 T. A smooth background has been subtracted from traces (b)-(d).

tum well is kept as impurity-free as possible through the use of undoped GaAs setback layers (700 Å on the emitter side and 200 Å on the collector side), located between the double barrier structure and the heavily doped ($n^+ = 2 \times 10^{18}$ cm^{-3}) contact layers (see Fig. 1). The as-grown wafers are etched to yield 100 μm diameter mesas, each a resonant tunneling diode; other details of the sample growth and characterization are given in Ref. [7].

The experimental procedure is to rotate the sample to a measured tilt angle θ ($\theta = 0°$ is a magnetic field perpendicular to the plane of the barriers, parallel to the direction of current flow). Resonant tunneling current-voltage (I-V) traces at a temperature of 1.5 K are recorded in 0.1 T magnetic field steps over a range from $B = 0$ to 12 T. All experimental data in the figures are from the 1200 Å well. Traces (a) and (b) in Fig. 1 are the same I-V data for $\theta = 27°$ at $B = 0$. In trace (b), a smooth background current is subtracted to emphasize the current peaks. The same procedure is applied at (c) $B = 6$ T and (d) $B = 12$ T. Note the amplification required to observe the peaks in these traces. Resonant tunneling spectroscopy enjoys a long history as a probe of the quantum well density of states [8]. A peak in an I-V trace evidences a corresponding peak in the quantum well density of states.

In Fig. 2 the voltages at which current peaks occur in the I-V traces are plotted as a function of the total magnetic field for five of eleven angles studied from $\theta = 0°$ to 45°. The peak positions are plotted as filled circles; the lines will be discussed with the model calculations. At $\theta = 0°$ [Fig. 2(a)], a tunneling peak occurs when the energy level in the 2DEG emitter aligns with the energy of a confinement subband in the quantum well. As expected, these subband peaks show no strong dependence on magnetic field. Note that at all nonzero tilt angles the data can be separated into regions with clearly defined boundaries. At $\theta = 11°$ [Fig. 2(b)], for example, most of the data resemble the subbands at $\theta = 0°$. Now, however, a doubling of the number of peaks occurs in two distinct regions of bias voltage versus magnetic field. These two regions gradually broaden and merge as the tilt angle is increased to $\theta = 27°$ [Fig. 2(c)]. Upon increasing the tilt angle to $\theta = 38°$ [Fig. 2(d)], the low field region remains subbandlike, followed by a narrow region of peak tripling and increasingly complicated peak structure at higher magnetic fields. Finally, at $\theta = 45°$ [Fig. 2(e)], there is a sharp transition between the subbandlike region and a disordered region.

To interpret these observations, we analyze the transition from regular to chaotic dynamics within the classical model described above. The electric field F, which arises from the applied bias voltage U (see Fig. 1) [9], is perpendicular to the walls; the applied magnetic field,

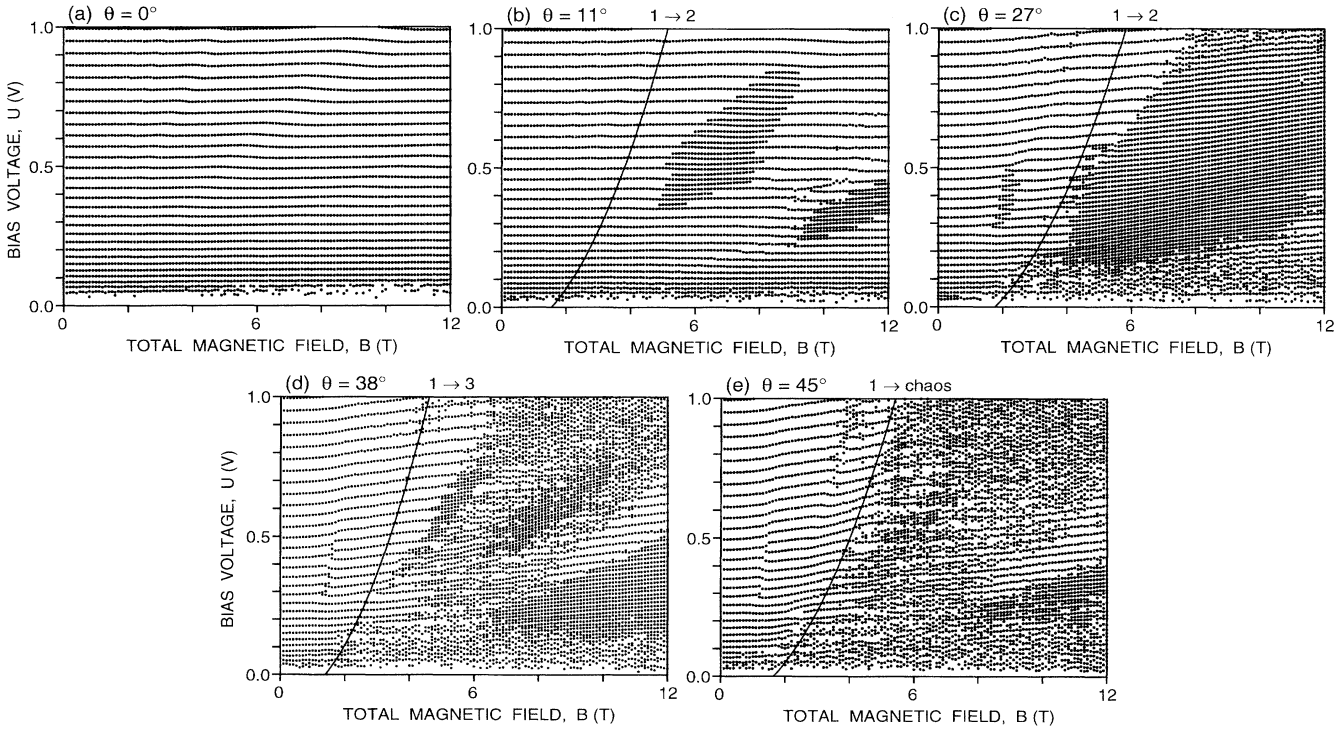

FIG. 2. Peak positions from the resonant tunneling I-V traces at $T = 1.5$ K as a function of total magnetic field. At (a) $\theta = 0°$: quantum well subbands; (b) $\theta = 11°$: two regions of peak doubling arise; (c) $\theta = 27°$: peak doubling regions have broadened and merged; (d) $\theta = 38°$: a narrow peak tripling region; and (e) $\theta = 45°$: direct transition to disordered peak positions. The solid lines are transition boundaries from Poincaré section calculations: at (b) $\theta = 11°$ and (c) 27°, a bifurcation; at (d) $\theta = 38°$, a trifurcation; and at (e) $\theta = 45°$, an abrupt order to chaos transition.

$\vec{B} = B\sin\theta\hat{y} + B\cos\theta\hat{z}$, is tilted. The resulting motion in three dimensions is governed by the Hamiltonian $H = (\mathbf{p} + e\mathbf{A})^2/2m^* - eFz$. Here we adopt the gauge $\mathbf{A} = (-By\cos\theta/2 + Bz\sin\theta, Bx\cos\theta/2, 0)$. By analogy with Landau's reduction of 2D cyclotron motion to a 1D harmonic oscillator, we choose canonical coordinates Q and P to reduce our problem to 2D [10].

$$H = \frac{P^2}{2m^*} + \frac{m^*\omega_c^2 Q^2}{2} + \frac{p_z^2}{2m^*} - eFz - (\omega_c\sin\theta)Qp_z\,. \quad (1)$$

This new Hamiltonian describes harmonic confinement in the Q direction (cyclotron in-plane motion) and a constant electric field with hard wall confinement in the z direction (bouncing motion). The last term couples these two motions. At zero tilt angle, the coupling term vanishes and the system is integrable.

It is convenient to employ natural units based on the effective mass of electrons in GaAs m^*, the cyclotron frequency ω_c, and the length $l \equiv m^*F/eB^2$. The unit of length is chosen to make the natural electric and magnetic energies equal: $eFl = m^*\omega_c^2 l^2$. In these units, the electric and magnetic field are both unity and the classical dynamics is determined solely by tilt angle θ, electron energy E and well width d. In natural units, these are given by θ, $E/(m^*F^2/B^2)$, and $d/(m^*F/eB^2)$, respectively. The classical mechanics remains constant so long as these parameters are unchanged in the natural units. For illustration, several isoclassical lines are superimposed on the data in Fig. 2. The isoclassical lines are roughly parabolic in shape because, to a good approximation, the electron is injected with an energy $E \sim U \sim F$ (see Fig. 1).

To visualize the complicated classical dynamics of this system we examine the Poincaré surface of section (PS). Particle trajectories are computed by analytically solving the equations of motion between specular collisions with the collector wall [11]. Following a given trajectory, a point is added to the PS at (P, Q) for the values of P and Q at each collision. Note that P and Q are (up to constant multiplicative factors) the electron's in-plane velocity components. Initial conditions for the PS calculations include all trajectories for which the kinetic energy of the electron at the collector barrier is given by the 2D emitter confinement energy plus the kinetic energy gain due to acceleration through the quantum well.

At zero tilt angle, the electron moves along a helix and the orbit traces out a circle in the PS. Thus at $\theta = 0°$, the PS is a pattern of concentric circles characteristic of a *stable* system. As tilt angle or magnetic field is increased, the motion grows progressively more chaotic. In the PS's, islands of regular motion are centered on stable periodic orbits, which are surrounded by a chaotic sea. As the system becomes more chaotic, the islands of integrability become smaller and disappear.

Although classical dynamics usually change gradually, occasionally a stable periodic orbit will abruptly bifurcate or trifurcate. Upon bifurcating, a stable periodic orbit [see Fig. 3(a)] loses stability and simultaneously gives birth to two stable periodic orbits with exactly twice the period time of the original orbit [see Fig. 3(b)]. When a stable orbit trifurcates, three new stable periodic orbits arise, each with thrice the original period [see Figs. 3(c) and 3(d)]. Bifurcations and trifurcations are well-established precursors to chaos [12].

To relate the classical mechanics to the data we use Gutzwiller's periodic orbit theory [1]. According to Gutzwiller's trace formula, the density of states for a chaotic system can be written as a sum over isolated unstable periodic orbits. Each periodic orbit contributes an oscillatory term with energy period h/T_P, where T_P is the period time of the orbit. A similar formula derived by Berry and Tabor [1] for regular systems shows that *stable* periodic orbits produce *larger* oscillations in the density of states. In the ideal case one should sum over periodic orbits of arbitrary duration; however, in the quantum well sample there is a subpicosecond cutoff, due to optical phonon emission [13]. If the quantum well is in a completely chaotic regime, the shortest *unstable* periodic orbits will determine the resonant tunneling spectra, as reported by Fromhold *et al.* [5]. However, in studying the transition between regular motion at low magnetic fields and completely chaotic motion at high magnetic fields, we expect that the observed *I-V* spectra (Fig. 1) will be dominated by the evolution of the *stable* periodic orbits.

This interpretation suggests that the sharp onset of peak doubling or tripling in the data can be understood in terms of the bifurcation [6] or trifurcation of stable periodic orbits. We test this three ways. First, the isoclassical bifurcation or trifurcation lines lie close to the onset of

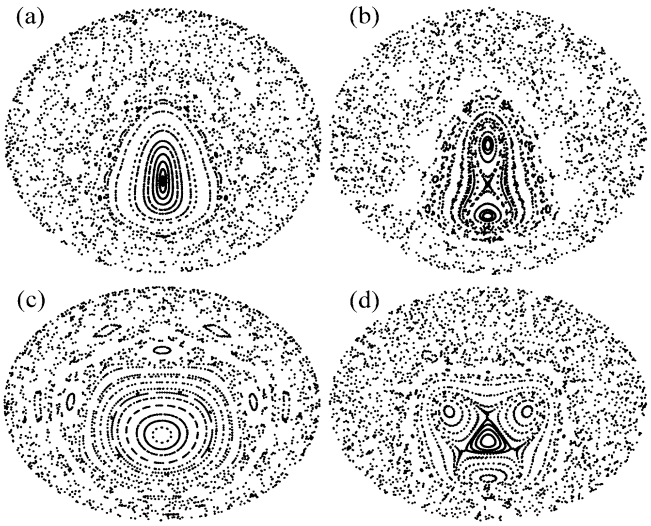

FIG. 3. Examples of Poincaré sections for the 1200 Å sample at $U = 0.5$ V showing (a) a stable periodic orbit at $\theta = 27°$ and $B = 4.2$ T undergoing (b) bifurcation at $B = 4.4$ T, yielding peak doubling shown in Fig. 2(c). (c) shows a stable periodic orbit at $\theta = 38°$ and $B = 3.0$ T undergoing (d) trifurcation at $B = 3.5$ T, yielding peak tripling shown in Fig. 2(d).

peak doubling or tripling regions. See, for example, the bifurcation boundaries (lines marked "1 → 2") in Fig. 2 at $\theta = 11°$ and 27°. At $\theta = 38°$, the bifurcation has given way to a trifurcation in the PS, consistent with the observation of a narrow region of peak *tripling* [line marked "1 → 3" in Fig. 2(d)].

As a second test, we compare the calculated stable orbit periods to the observed peak spacings. For example, at $\theta = 11°$ and $U = 0.5$ V, the calculated periodic orbit time is 0.23 ps for magnetic fields below the bifurcation. This corresponds to $\Delta U = 39$ mV [9], in good agreement with the observed peak spacing in Fig. 2(b). Upon bifurcation, the stable orbit period doubles and the observed peak spacing halves. Quantitative agreement within 15% is typically obtained at all tilt angles studied for all four samples.

A third test comes from comparison of data at a fixed tilt angle for the four samples of different well width. In our interpretation, the locations of the transitions are determined entirely by the *classical* variables. There is no $\hbar$ dependence. Thus, for example, the trifurcation onset should scale roughly as the inverse of the quantum well width. This follows from classical scaling in terms of the natural units discussed previously, together with the approximation that $F \sim U/d$. Table I indicates that the trifurcation onset does indeed scale classically, even for quantum well widths as small as 400 Å. This, along with the parabolic magnetic-field dependences in the Fig. 2 data, establishes classical scaling in a condensed matter system [14].

So far, we have focused on transitions in the data at low magnetic field. The dynamics of stable periodic orbits account for some of the dominant features seen at higher magnetic fields as well. For example, the PS's at 11° find a restabilization of the original periodic orbit ~2 T above the bifurcation boundary of Fig. 2(b) [15]. A second bifurcation in the PS's accounts for the second observed peak doubling region. At 27°, the PS's do find a single wide peak doubling region, although the calculated width is only half the observed width; a transition to chaos is found in the PS's which is not evidenced in the data. Finally, at 38° and 45°, the reemergence of an ordered subbandlike region at the highest fields ($B \gtrsim 10$ T for $U \sim 0.5$ V) corresponds to the reemergence of a stable island from the chaotic sea in the PS calculations.

TABLE I. Magnetic field B_{tri} of observed trifurcation at $U = 0.5$ V for four different quantum well widths d. At each tilt angle θ confirmation of classical scaling ($B_{\text{tri}} \sim 1/d$) is found, where $B^* = [d/(120\ \text{nm})]B_{\text{tri}}$.

	$\theta = 38°$				$\theta = 45°$			
d(nm)	40	60	85	120	40	60	85	120
B_{tri}(T)	11.6	8.3	5.7	4.4	12.0	9.5	6.2	5.0
B^*(T)	3.9	4.2	4.0	4.4	4.0	4.8	4.4	5.0

In conclusion, we report a distinct transition from order to chaos in a quantum well. Poincaré section calculations find quantitative agreement with the roughly parabolic magnetic field dependence of the transition. We directly observe stable orbit bifurcations and trifurcations and identify these as the precursors of the transition to chaos.

We thank H. Baranger, O. Narayan, and D. Ullmo for discussions and D. Shepelyansky and A. D. Stone for pointing out the importance of bifurcations in this system. G. M. thanks the Max-Planck-Gesellschaft for financial support via the Otto-Hahn-Medaille.

*Present address: Philips Research Laboratories, Prof. Holstlaan 4, 5656 AA Eindhoven, The Netherlands.

[1] For a survey of theory, see M. C. Gutzwiller, *Chaos in Classical and Quantum Mechanics* (Springer, Berlin, 1990).

[2] For a review, see D. Delande, in *Chaos & Quantum Physics,* edited by M. J. Giannoni, A. Voros, and J. Zinn-Justin (North-Holland, New York, 1991).

[3] D. Weiss *et al.,* Phys. Rev. Lett. **70**, 4118 (1993); R. Schuster *et al.,* Phys. Rev. B **49**, 8510 (1994).

[4] C. M. Marcus *et al.,* Phys. Rev. Lett. **69**, 506 (1992); M. W. Keller *et al.,* Surf. Sci. **305**, 501 (1994); A. M. Chang *et al.,* Phys. Rev. Lett. **73**, 2111 (1994).

[5] T. M. Fromhold *et al.,* Phys. Rev. Lett. **72**, 2608 (1994).

[6] D. L. Shepelyansky and A. D. Stone, Phys. Rev. Lett. **74**, 2098 (1995).

[7] G. S. Boebinger *et al.,* Phys. Rev. B **47**, 16 608 (1993).

[8] See, e.g., L. Eaves, in *Electronic Properties of Multilayers and Low-Dimensional Semiconductor Structures,* edited by J. M. Chamberlain *et al.* (Plenum Press, New York, 1990), and references therein.

[9] Measurement (see Ref. [7]) of the voltage dependence of the 2DEG emitter electron density for $U \gtrsim 0.2$ V yields $F = (5.9U + 0.6) \times 10^6$ V/m (U in volts) for the 1200 Å sample. From this and sample dimensions, we conclude that two peaks separated by ΔU are $\sim 0.47 e\Delta U$ apart in energy.

[10] The transformation is $P = p_x + eA_x$, $Q = (p_y + eA_y)/eB\sin\theta$, and $p_z \rightarrow p_z - eQB\cos\theta$.

[11] Shepelyansky and Stone [6] introduced a computationally simpler model based on Eq. (1) in which the emitter barrier is removed, since few trajectories impact the emitter barrier. We have used this in Figs. 2 and 3 and verified that a double barrier calculation also agrees with our data.

[12] L. E. Reichl, *The Transition to Chaos* (Springer-Verlag, New York, 1992), Chap. 3.

[13] E. M. Conwell, *High Field Transport in Semiconductors,* Solid State Physics: Advances in Research and Applications, edited by H. Ehrenreich, F. Seitz, and D. Turnbull (Academic, New York, 1967), Suppl. 9.

[14] For classical scaling in atomic systems, see, e.g., B. E. Sauer, M. R. W. Bellerman, and P. M. Koch, Phys. Rev. Lett. **68**, 1633 (1992).

[15] G. S. Boebinger *et al.,* Surf. Sci. (to be published).